

Electronic Excited States of Si(100) and Organic Molecules Adsorbed on Si(100)

Nicholas A. Besley* and Adam J. Blundy

School of Chemistry, University of Nottingham, University Park, Nottingham, NG7 2RD, United Kingdom

Received: September 14, 2005; In Final Form: December 4, 2005

The electronically excited states of the Si(100) surface and acetylene, benzene, and 9,10-phenanthrenequinone adsorbed on Si(100) are studied with time-dependent density functional theory. The computational cost of these calculations can be reduced through truncation of the single excitation space. This allows larger cluster models of the surface in conjunction with large adsorbates to be studied. On clean Si(100), the low-lying excitations correspond to transitions between the π orbitals of the silicon–silicon dimers. These excitations are predicted to occur in the range 0.4–2 eV. When organic molecules are adsorbed on the surface, surface \rightarrow molecule, molecule \rightarrow surface, and electronic excitations localized within the adsorbate are also observed at higher energies. For acetylene and benzene, the remaining $\pi\pi^*$ excitations are found to lie at lower energies than in the corresponding gas-phase species. Even though the aromaticity of 9,10-phenanthrenequinone is retained, significant shifts in the $\pi\pi^*$ excitations of the aromatic rings are predicted. This is in part due to structural changes that occur upon adsorption.

Introduction

The silicon (100) surface is one of the most extensively studied systems in surface science and it has been the focus of a very large number of theoretical and experimental investigations. References 1–12 provide illustrative examples of this work. In addition to being a system of fundamental chemical interest, the Si(100) surface also plays a critical role in the processing of microelectronic devices. In recent years, there has been increasing interest in organic molecules covalently bonded to the surface. The combination of organic molecules and the Si(100) surface opens up the possibility of integrating the wide variety of functionalities of organic molecules with existing microelectronics technology. This has many potential applications, such as molecular electronics and chemical sensors.^{13–15}

The Si(100) surface undergoes a characteristic (2×1) reconstruction in which adjacent atoms pair, resulting in rows of Si=Si dimers. Multireference configuration interaction calculations have estimated the energy gain from dimer formation to be 1.75 eV.¹⁶ There has been some debate over if these dimers are “symmetric” or “buckled”. Spectroscopic data supported buckled dimers.^{17–21} Scanning tunneling microscope (STM) experiments at room temperature indicated symmetric dimers,²² while STM images at low temperatures showed buckled dimers.^{23,24} Currently, it is thought that the dimers are buckled, but at room temperature oscillation between the two buckled structures will occur at a frequency beyond the time resolution of STM experiments. However, recent STM images at very low temperatures predict the symmetric dimer with asymmetric dimers observed only near defects.²⁴ Among theoretical groups there has also been considerable debate regarding this issue.^{25–28} A recent paper has clarified many of the technical arguments.²⁸ Density functional theory (DFT) and quantum Monte Carlo calculations predict the buckled structure to be the lowest in energy, while multireference wave function methods favor the symmetric structure. Furthermore, restricted DFT calculations find the symmetric structure to be a saddle point, while spin-unrestricted calculations find the symmetric structure to be a minimum (although higher in energy than the minimum corresponding to the buckled structure). However, a

full resolution of this problem has yet to be achieved, since these calculations are based largely on finite models of the surface.

The Si=Si double bonds of the Si(100) surface are much weaker than C=C double bonds or molecular Si=Si double bonds. These weak bonds make the surface reactive toward the adsorption of molecules because stronger bonds are formed, resulting in an energetically favorable process.²⁹ Theoretical studies of a wide range of organic molecules, such as acetylene,¹⁰ ethene,³⁰ benzene,^{6,11,31} acrylonitrile,⁸ and thiophene,³² have been reported. In general, previous work has focused on the ground state of the adsorbed molecule, characterizing geometries and evaluating binding energies. Recently, we have begun to study the excited states of molecules adsorbed on surfaces.^{33,34} Electronic excitations play an important role in surface science. They can be used to promote chemical reactions or photodesorption. Furthermore, the characterization of the structure of surfaces and adsorbed monolayers is a fundamental challenge. The study of excited states also provides valuable information that can assist in the characterization of an organic surface layer.³⁵

The lowest lying (triplet) excited state of the Si(100) surface has been studied by using DFT with the B3LYP exchange correlation functional and 6-311+G* basis set.³⁶ The energy difference between the optimal ground-state structure and optimized triplet state structure was found to be 0.34 and 0.38–0.40 eV for the Si₉H₁₂ and Si₂₁H₂₀ clusters, respectively. The vertical excitation energy was reported to be 0.79 eV for a single dimer cluster model. The results from DFT were shown to be consistent with predictions from complete active space self-consistent field with second-order perturbation theory.³⁶ It was concluded that the energy difference between the two states was sufficiently small for a significant population of the upper state under common conditions. The optical absorption spectra of hydrogenated silicon clusters have also been studied. The interest in these systems arises from their role as a prototypical model for quantum-confined semiconductor systems. Time-dependent density functional theory (TDDFT) and the Bethe–Salpeter equation were applied to study a range of cluster sizes. For larger

clusters, the methods gave similar gross features, although very different results were obtained for the smallest (SiH_4) cluster.³⁷

Reflectance anisotropy (or difference) spectroscopy (RAS or RDS) measures the relative difference in the reflectances of two orthogonal crystallographic axes of a surface, and is a valuable tool for characterizing the surfaces of crystalline materials.³⁸ The structure of the Si(100) surface has been studied with RDS.^{39–42} For the bare Si(100) surface, features in the RDS spectra below 2 eV are associated with electronic transitions of the Si=Si dimers.⁴⁰ The use of RDS to study thin organic layers is an emerging area of research. The first observation of intramolecular transitions of adsorbed molecules in RDS was reported in a study of 9-anthracene carboxylic acid on Cu(110).³⁵ Recently, Hacker and Hamers have studied the RDS of organic molecules adsorbed on the Si(100) surface.⁴³ The RDS spectra of a 9,10-phenanthrenequinone monolayer had a strong band at 5.2 eV that was absent in the corresponding spectra for 1,2-cyclohexanedione. This feature was assigned to a $\pi\pi^*$ transition within the 9,10-phenanthrenequinone molecule. Recent calculations have questioned this assignment, and assign this feature to adsorption-induced distortions of the substrate.^{44,45} Understanding RDS spectra requires a correspondence between spectral features and the underlying electronic transitions. Consequently, theoretical calculations of the excited states of adsorbed molecules can play an important role in the interpretation of RDS spectra. Furthermore, these calculations can identify suitable molecules with intramolecular transitions within the 1.5–5.5 eV energy range accessible to the technique.³⁵

In this paper, we demonstrate how quantum chemistry can be applied to study the excited states of the Si(100) surface and adsorbed organic layers. This represents a first principles determination of the electronic spectra of these systems. Our calculations employ a recently developed TDDFT formalism³³ and use cluster models of the Si(100) surface. We report calculations of the bare Si(100) surface and ethyne, benzene, and 9,10-phenanthrenequinone adsorbed on the Si(100) surface. Electronic excitations that are charge transfer in nature, in addition to local surface and adsorbant excitations, are characterized and the implications for reported RDS measurements of organic layers discussed.

Computational Details

TDDFT provides an accurate prediction of excitation energies and oscillator strengths at a relatively low computational cost.⁴⁶ Despite the computational efficiency of TDDFT, the study of the excited states of molecules adsorbed on a surface remains a challenge. This is due to bulk surface excitations that are significantly lower in energy than the valence molecular excitations of adsorbed species. Consequently, if large clusters are used to model the surface, the molecular excited states become prohibitively expensive to compute. We have recently introduced a scheme that overcomes this problem by restricting the TDDFT calculation to a subset of the single excitation space including single excitations between a subset of the occupied and virtual orbitals.³³ The selection of the orbital subsets is based on an analysis of the Mulliken populations⁴⁷ and molecular orbital coefficients for the occupied and virtual orbitals, respectively. A parameter κ_i^{occ} is defined such that

$$\kappa_i^{\text{occ}} = \sum_{\lambda} M_{\lambda i} \quad (1)$$

where $M_{\lambda i}$ is the contribution to the Mulliken population of orbital i from basis function λ . The summation runs over the

basis functions centered on atoms in a defined region of the system. Thus κ_i^{occ} provides a measure of the extent that orbital i is localized in this region. All κ_i^{occ} are evaluated; if κ_i^{occ} is greater than a user defined value (between 0 and 2) then excitations from the orbital i are included in the truncated single excitation space. A similar scheme based on the normalized molecular orbital coefficients is used for the virtual orbitals.

$$\kappa_a^{\text{vir}} = \sum_{\lambda} |C_{\lambda a}|^2 \quad (2)$$

Similarly, if κ_a^{vir} is sufficiently large, excitations to these orbitals are included. Through this method the electronic excitations within a local region of a system can be studied. This approach has been applied to the study of CO on the Pt-(111) surface³⁴ and its success depends on there being a weak coupling between the electronic excitations of interest and those excluded from the excitation subspace.

In this study, the extended surface is modeled by using finite clusters with open valencies capped by hydrogen. These clusters are depicted in Figure 1. The focus of this study is the excited states of the Si(100) surface with molecular adsorbates. Fully characterized quantitative structural information of these systems from experiment is not available. Consequently, we have used structures optimized using DFT with the hybrid B3LYP exchange-correlation functional⁴⁸ and 6-31G* basis set.^{49,50} For consistency, we have also used B3LYP/6-31G* structures for the models of the bare surface. The predicted Si=Si bond length in all clusters (except Si_2H_4) is 2.22 Å. This is within the error of the experimental value of 2.26 ± 0.1 Å.⁵¹ It is possible to perform more comprehensive geometry optimizations in which lower layers are frozen in bulk orientations and upper layers allowed to relax. However, such constrained optimizations have been shown to consistently give Si=Si dimer bond lengths that are significantly longer than experiment.²⁵ The clusters we have used in this study have a symmetric dimer configuration. The subtle differences between the symmetric and buckled dimer configurations should not have a very large effect on the calculated excited states. Furthermore, once a molecule is adsorbed on the surface, it is unclear whether the surrounding Si=Si dimers will be symmetric or buckled.

Excitation energies and intensities are computed with TDDFT exploiting the Tamm–Dancoff approximation⁵² (TDA) implemented in the Q-CHEM software package.⁵³ The B3LYP functional in conjunction with the 6-31+G* basis set was used for these calculations. We have found that this combination represents a good compromise between accuracy, computational cost, and stability with respect to convergence of the self-consistent field calculation. For the acetylene system, the sensitivity to basis set is explored in more detail. TDDFT with the B3LYP functional does have well-known limitations,⁵⁴ and these are discussed in the context of the current study.

Results and Discussion

Excitations of the Si(100) Surface. The computed vertical singlet and triplet excitation energies associated with the Si=Si dimers of the Si(100) surface for the different cluster models of the surface are shown in Table 1. For Si_2H_4 , this excitation will clearly be a $\pi\pi^*$ transition. For the larger clusters, the corresponding orbitals remain essentially π -like in nature, with lobes predominantly above and below the Si=Si dimers. These orbitals are shown for the $\text{Si}_{21}\text{H}_{20}$ cluster in Figure 2. Consequently, these excitations are also denoted $\pi\pi^*$. For all the cluster models studied, these excitations are the lowest in energy.

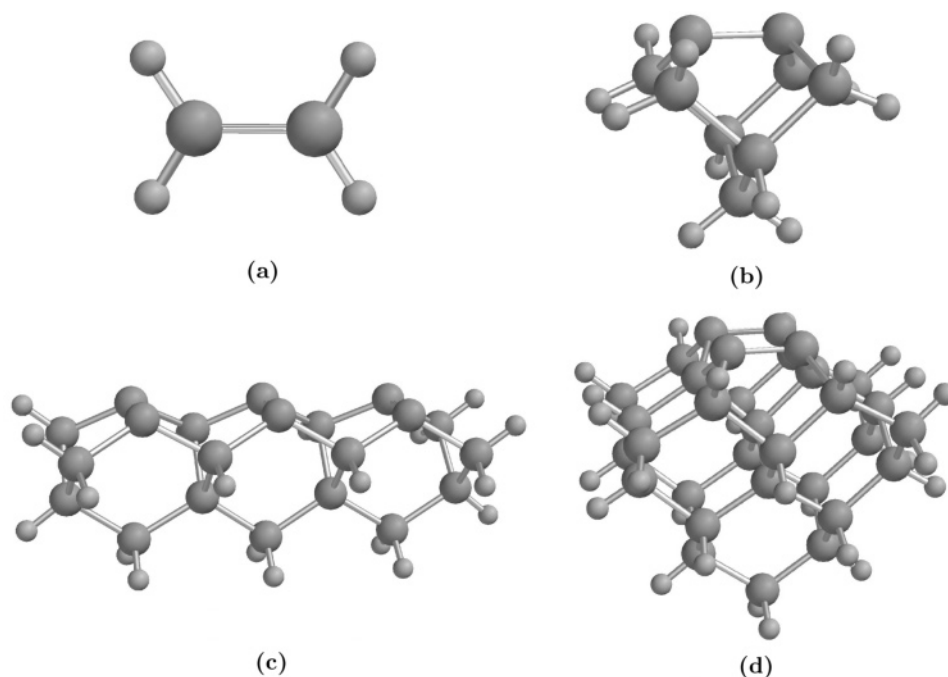


Figure 1. Models of the Si(100) surface: (a) Si₂H₄, (b) Si₉H₁₂, (c) Si₂₁H₂₀, and (d) Si₃₂H₂₈.

TABLE 1: $\pi\pi^*$ Excitation Energies for Si(100)^a

transition	triplet states				singlet states			
	Si ₂ H ₄	Si ₉ H ₁₂	Si ₂₁ H ₂₀	Si ₃₂ H ₂₈	Si ₂ H ₄	Si ₉ H ₁₂	Si ₂₁ H ₂₀	Si ₃₂ H ₂₈
$\pi_0 \rightarrow \pi^*_0$	1.94	0.76	0.40	0.42	4.56 (0.46)	2.59 (0.09)	1.15	1.13
$\pi_0 \rightarrow \pi^*_{+1}$			1.30	1.35			1.45	1.96 (0.04)
$\pi_0 \rightarrow \pi^*_{+2}$			1.41				2.12 (0.04)	
$\pi_{-1} \rightarrow \pi^*_0$			0.56	0.53			1.25	1.38
$\pi_{-1} \rightarrow \pi^*_{+1}$			0.60	1.48			1.81	2.05
$\pi_{-1} \rightarrow \pi^*_{+2}$			1.90				1.86	
$\pi_{-2} \rightarrow \pi^*_0$			1.45				1.46	
$\pi_{-2} \rightarrow \pi^*_{+1}$			1.49				2.23	
$\pi_{-2} \rightarrow \pi^*_{+2}$			1.93				2.23 (0.05)	

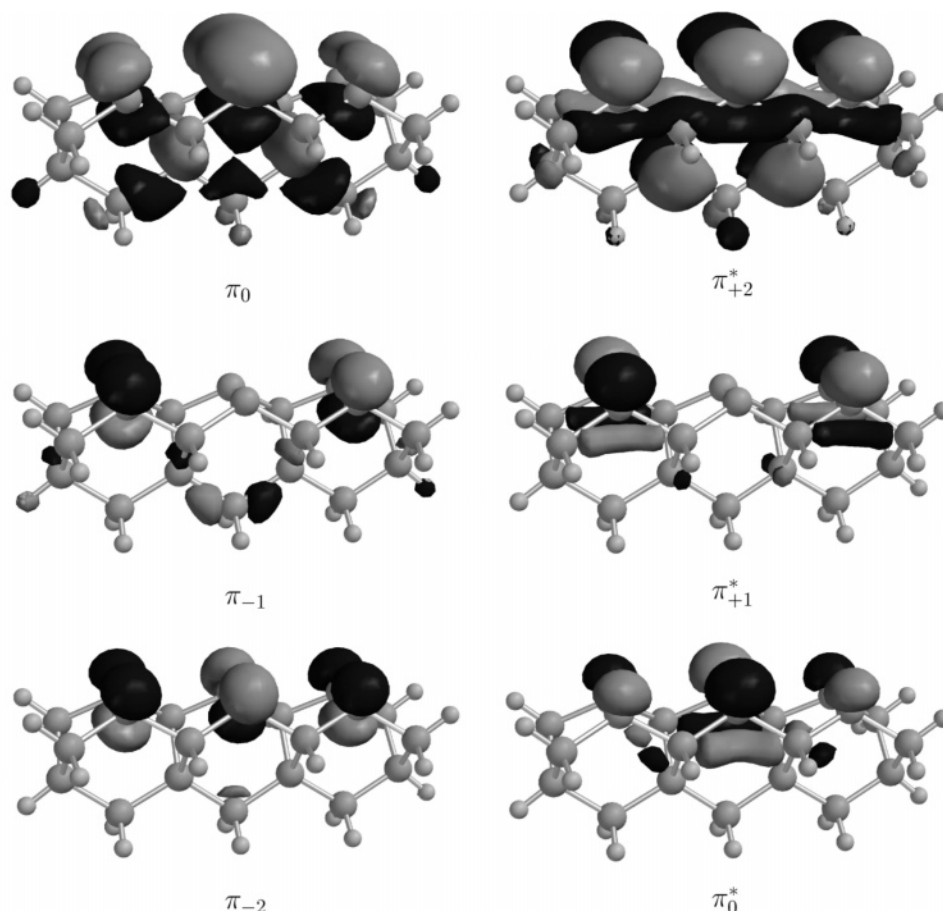
^a Oscillator strengths greater than 0.01 are given in parentheses.

The simplest surface models Si₂H₄ and Si₉H₁₂ have one Si=Si dimer, and consequently one $\pi\pi^*$ excitation corresponding to the HOMO (π_0) to LUMO (π^*_0) excitation. For singlet and triplet states, the predicted $\pi\pi^*$ excitation energy is considerably lower (by 1–2 eV) for the Si₉H₁₂ cluster. This change is likely to be associated with the increase in the Si=Si bond length from 2.14 Å in Si₂H₄ to 2.22 Å in the cluster. Excitation energies of 0.76 and 2.59 eV are predicted for the triplet and singlet states in the Si₉H₁₂ cluster, respectively. The triplet excitation energy of 0.76 eV is very close to the 0.79 eV reported in earlier work.³⁶ Throughout this study we report vertical excitation energies. These are an upper bound to the adiabatic excitation energies. Since significant relaxation of the excited state may occur,³⁶ the vertical excitation energies are likely to be a few tenths of an electronvolt higher than the adiabatic values.

These smaller systems are also accessible to multireference configuration interaction (MRCI) calculations. With an active space consisting of the HOMO and LUMO orbitals, MRCI in conjunction with the 6-31+G* basis set predicts excitation energies of 2.02 and 5.49 eV for the triplet and singlet $\pi\pi^*$ excitations in Si₂H₄, respectively. For the Si₉H₁₂ cluster, corresponding values of 0.81 and 3.05 eV are obtained. The values for the triplet state are in good agreement with the predictions from TDDFT. However, there are large differences for the singlet state. With a larger basis set, aug-cc-pVDZ, we find values of 2.09, 4.56, 0.83, and 2.92 eV for the singlet and

triplet states of Si₂H₄ and Si₉H₁₂, respectively. For the better quality basis set there is closer agreement between the MRCI values and TDDFT. The trend also suggests this agreement will improve for more complete basis sets. This gives some confidence that TDDFT provides an adequate treatment of this system.

The larger surface models have more than one Si=Si dimer. The π orbitals associated with these dimers are not localized on a single dimer but are delocalized over the silicon dimers. For the Si₂₁H₂₀ cluster, these are the HOMO (π_0), HOMO-1 (π_{-1}), HOMO-2 (π_{-2}), LUMO (π^*_0), LUMO+1 (π^*_{+1}), and LUMO+2 (π^*_{+2}) orbitals. The computed transition energies for excitations between these orbitals are also included in Table 1. For both triplet and singlet states there is a large reduction in the HOMO \rightarrow LUMO ($\pi_0 \rightarrow \pi^*_0$) excitation energy compared with that of the smaller clusters. The remaining $\pi\pi^*$ excitations lie in the range 0.5–2.25 eV. Of these excitations, some of the excitations to singlet states have significant intensity. These results are consistent with the observation in experiment of a peak near 1.4 eV in the RDS spectrum, which was attributed to the silicon dangling bonds in Si(100).⁴⁰ There is little change in the $\pi_0\pi^*_0$ excitation energy for the larger Si₃₂H₂₈ cluster. This provides some indicative evidence that convergence of the excitation energies with respect to sublayers of the cluster has been achieved. The clusters used in this study involve only one row of dimers. The interactions between inter-row dimers are

**Figure 2.** π orbitals of $\text{Si}_{21}\text{H}_{20}$.

expected to be small since the interdimer distance is much larger than the distance between dimers in the same row.³⁶ Our preliminary calculations on a cluster including two dimers from adjacent rows show that the triplet and singlet $\pi_0\pi_0^*$ excitation energies lie at 0.82 and 1.94 eV, respectively. These are larger than those for the corresponding excitations within a dimer row. Above the $\pi\pi^*$ excitations are a large number of $\sigma \rightarrow \pi^*$ and $\pi \rightarrow \sigma^*$ excitations; however, in this paper we confine our analysis to $\pi\pi^*$ -like transitions.

Acetylene Adsorbed on the Si(100) Surface. The predicted C–C and Si–Si bond lengths once acetylene is adsorbed on the surface are 1.35 and 2.34 Å, respectively. These are in agreement with the experimental estimates of 1.32–1.37 and 2.44 ± 0.58 Å. Table 2 shows computed excitation energies of acetylene adsorbed on the models of the Si(100) surface. Adsorption of acetylene on Si_2H_4 and the Si_9H_{12} cluster saturates the Si=Si double bond, and the only π orbitals remaining are those associated with acetylene. The computed triplet and singlet $\pi_{\text{C}_2\text{H}_2} \rightarrow \pi_{\text{C}_2\text{H}_2}^*$ excitation energies are 4.22 and 6.31 eV, and 3.81 and 4.92 eV for Si_2H_4 and Si_9H_{12} , respectively. For gas-phase acetylene, B3LYP/6-31+G* predicts excitation energies of 5.37 and 5.90 eV for the $^3\pi\pi^*$ states and 7.10 and 7.20 eV for the $^1\pi\pi^*$ states. Furthermore, values of 4.41 and 7.83 eV are obtained for the triplet and singlet $\pi\pi^*$ excitations of gas-phase ethene. This clearly indicates that there is a significant decrease in the $\pi\pi^*$ excitation energies on adsorption. For these systems, we have also computed excitation energies with the aug-cc-pVDZ basis set. Using this basis set, excitation energies of 4.22 and 6.24 eV for acetylene on Si_2H_4 and 3.82 and 4.89 eV for Si_9H_{12} are obtained. The predicted transition energies obtained by using the larger basis set are within 0.1 eV of the values obtained with 6-31+G*. Since there are likely to be larger

TABLE 2: $\pi\pi^*$ Excitation Energies of Acetylene on Si(100)^a

transition	triplet	singlet
Si_2H_4		
$\pi_{\text{C}_2\text{H}_2} \rightarrow \pi_{\text{C}_2\text{H}_2}^*$	4.22	6.31 (0.02)
Si_9H_{12}		
$\pi_{\text{C}_2\text{H}_2} \rightarrow \pi_{\text{C}_2\text{H}_2}^*$	3.81	4.93 (0.01)
$\text{Si}_{21}\text{H}_{20}$		
$\pi_{\text{Si}_1} \rightarrow \pi_{\text{Si}_1}^*$	0.64	1.73
$\pi_{\text{Si}_1} \rightarrow \pi_{\text{Si}_2}^*$	0.66	1.79
$\pi_{\text{Si}_1} \rightarrow \pi_{\text{C}_2\text{H}_2}^*$	3.18	3.24
$\pi_{\text{Si}_2} \rightarrow \pi_{\text{Si}_1}^*$	1.79	2.14 (0.07)
$\pi_{\text{Si}_2} \rightarrow \pi_{\text{Si}_2}^*$	1.80	2.17
$\pi_{\text{Si}_2} \rightarrow \pi_{\text{C}_2\text{H}_2}^*$	3.44	3.46
$\pi_{\text{C}_2\text{H}_2} \rightarrow \pi_{\text{Si}_1}^*$	2.85	3.11
$\pi_{\text{C}_2\text{H}_2} \rightarrow \pi_{\text{Si}_2}^*$	3.49	3.56
$\pi_{\text{C}_2\text{H}_2} \rightarrow \pi_{\text{C}_2\text{H}_2}^*$	3.82	5.07 (0.01)
$\text{Si}_{32}\text{H}_{28}$		
$\pi_{\text{Si}_1} \rightarrow \pi_{\text{Si}_1}^*$	0.54	1.82 (0.02)
$\pi_{\text{Si}_1} \rightarrow \pi_{\text{C}_2\text{H}_2}^*$	2.93	2.98
$\pi_{\text{C}_2\text{H}_2} \rightarrow \pi_{\text{Si}_1}^*$	2.63	2.73
$\pi_{\text{C}_2\text{H}_2} \rightarrow \pi_{\text{C}_2\text{H}_2}^*$	3.75	4.32

^a Oscillator strengths greater than 0.01 are given in parentheses.

sources of error, such as the exchange correlation functional, it is reasonable to proceed with the more modest 6-31+G* basis set.

The π -like orbitals of acetylene adsorbed on the $\text{Si}_{21}\text{H}_{20}$ cluster are shown in Figure 3. The HOMO and HOMO-1 orbitals are localized on the Si=Si dimers and have no contribution from acetylene. These orbitals have similar energies, with the HOMO-1 orbital 0.2 eV below the HOMO. The π orbital localized on acetylene lies significantly lower in energy, 1.9 eV below the HOMO. There is a similar pattern for the

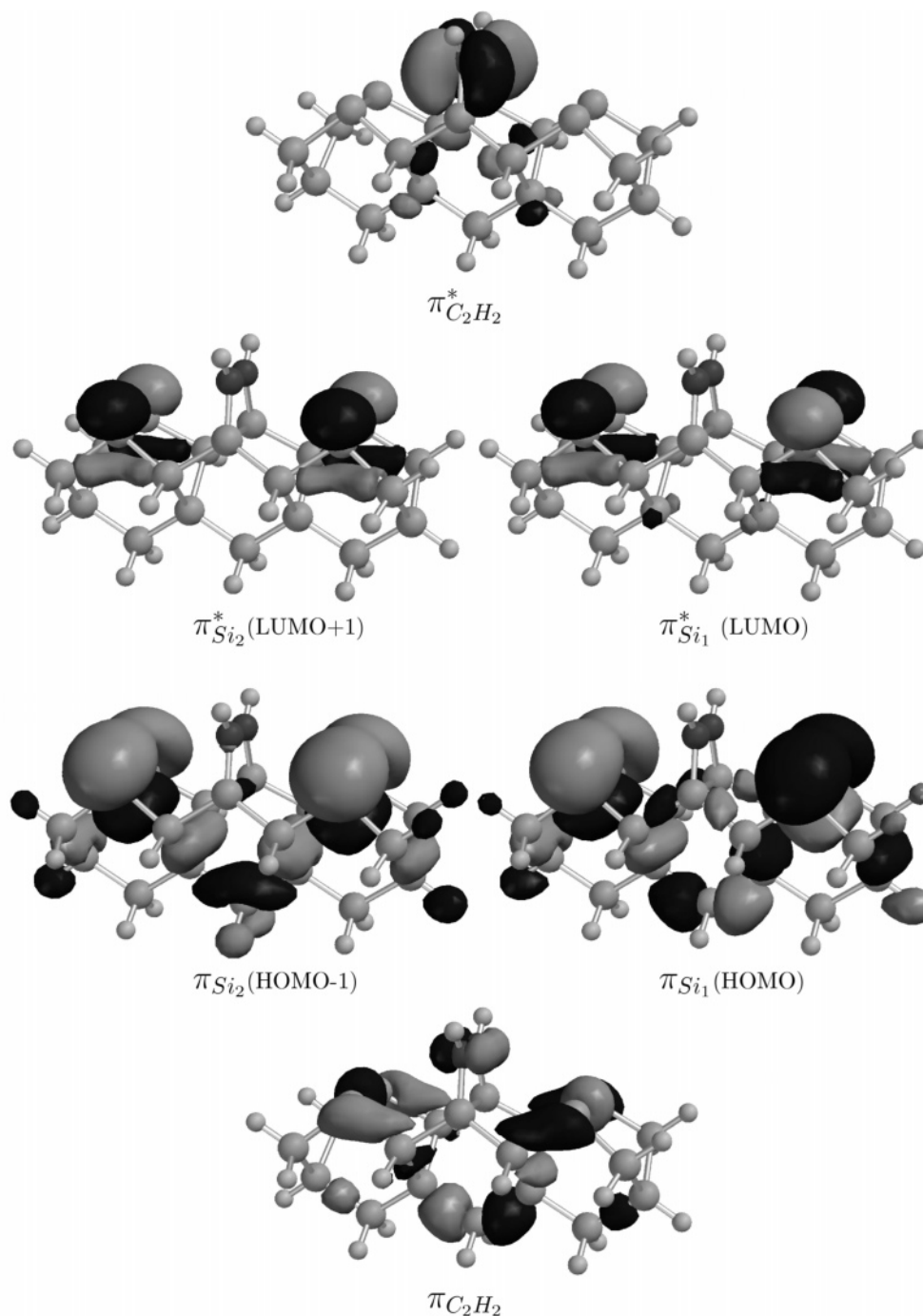


Figure 3. π orbitals of acetylene on $Si_{21}H_{20}$.

antibonding orbitals. The LUMO and LUMO+1 are localized on the Si=Si dimers and the π^* orbital of the acetylene is much higher in energy. The calculated $\pi_{C_2H_2} \rightarrow \pi_{C_2H_2}^*$ excitation energy for acetylene on the $Si_{21}H_{20}$ cluster is 5.07 eV. This is close to the computed value for the Si_9H_{12} cluster. There is a significant decrease in the predicted $\pi_{C_2H_2} \rightarrow \pi_{C_2H_2}^*$ excitation energy for acetylene on the large $Si_{32}H_{28}$ cluster. This shows that the excitation energies are sensitive to the cluster model. Examination of the adsorbed acetylene structure shows C–C, Si–C, and Si–Si bonds lengths of 1.35, 1.91, and 2.34 Å, respectively, for the $Si_{21}H_{20}$ cluster. Corresponding values for the $Si_{32}H_{28}$ cluster are 1.35, 1.91, and 2.36 Å. It is probably unlikely that the change in excitation energy is associated with these small differences. A possible origin of this difference may be that in the larger cluster there is “surface” on only one side of acetylene.

For the two larger clusters, transitions associated with Si=Si dimers and excitations between the surface and adsorbed C_2H_2 are observed. After the adsorption of C_2H_2 , there is an increase in the band gap, and correspondingly an increase in the remaining intrasurface $\pi_{Si} \rightarrow \pi_{Si}^*$ excitation energies. For the $Si_{21}H_{20}$ cluster, these are predicted to lie at ~ 0.65 and 1.8 eV for the triplet states and ~ 1.8 and 2.15 eV for the singlet states. Excitations from the surface π_{Si} orbitals to the $\pi_{C_2H_2}^*$ orbital can be identified, and are predicted to lie at 3.24 and 3.46 eV for singlet spin. The corresponding triplet states are only slightly lower in energy. Excitations from the $\pi_{C_2H_2}$ orbital to the π_{Si}^* orbitals are also observed, and lie at 3.11 and 3.56 eV for singlet spin. On the larger $Si_{32}H_{28}$ cluster, there is a decrease in the transition energies for these excitations. These transitions can be regarded as charge transfer in nature. For this type of transition, TDDFT can often predict excitation energies that are

TABLE 3: Predicted Singlet Excitation Energies for Acetylene on Si₂₁H₂₀ with Different Truncation Schemes^a

transition	full	C ₂ H ₂	C ₂ H ₂ + 2Si	Si=Si	C ₂ H ₂ + Si=Si	C ₂ H ₂ + Si=Si*
$\pi_{\text{Si}_1} \rightarrow \pi_{\text{Si}_1}^*$	1.73			1.76	1.74	1.75
$\pi_{\text{Si}_1} \rightarrow \pi_{\text{Si}_2}^*$	1.79			1.79	1.79	1.79
$\pi_{\text{Si}_1} \rightarrow \pi_{\text{CC}_2\text{H}_2}^*$	3.24			3.24	3.25	3.25
$\pi_{\text{Si}_2} \rightarrow \pi_{\text{Si}_1}^*$	2.14 (0.07)			2.51 (0.22)	2.32 (0.14)	2.33 (0.14)
$\pi_{\text{Si}_2} \rightarrow \pi_{\text{Si}_2}^*$	2.17			2.50	2.31	2.33
$\pi_{\text{Si}_2} \rightarrow \pi_{\text{C}_2\text{H}_2}^*$	3.46			3.45	3.46	3.46
$\pi_{\text{C}_2\text{H}_2} \rightarrow \pi_{\text{Si}_1}^*$	3.11	3.30	3.30		3.14	3.13
$\pi_{\text{C}_2\text{H}_2} \rightarrow \pi_{\text{Si}_2}^*$	3.56	3.43	3.43		3.57	3.57
$\pi_{\text{C}_2\text{H}_2} \rightarrow \pi_{\text{C}_2\text{H}_2}^*$	5.07 (0.01)	5.18	5.17		5.15 (0.05)	5.15 (0.05)

^a Full \Rightarrow no truncation; C₂H₂ \Rightarrow only excitations from orbitals localized on acetylene; C₂H₂ + 2Si \Rightarrow only excitations from orbitals localized on acetylene and the two silicon atoms to which they are bonded; Si=Si \Rightarrow only excitations from orbitals localized on the four silicon atoms of the Si=Si dimers; C₂H₂ + 4Si \Rightarrow only excitations from orbitals localized on acetylene and the four silicon atoms of the Si=Si dimers; C₂H₂ + Si=Si* \Rightarrow same as C₂H₂ + 4Si but with additional truncation in virtual space. Oscillator strengths greater than 0.01 are given in parentheses.

too low. This is a result of the local nature of the exchange correlation potential.⁵⁴ This is particularly the case for generalized gradient approximation (GGA) functionals. However, hybrid functionals, such as the one used here, do provide an improved description of charge-transfer excitations. More recent long-range corrected GGA functionals^{55,56} give a further improvement in the description of charge transfer excitations; we are currently implementing these functionals within our code. In summary, for acetylene on Si(100) our calculations predict three sets of π -like excitations. At low energies of 0.5–2 eV there are intrasurface excitations associated with the silicon dimers, above this in the range 2–4 eV are surface \rightarrow acetylene and acetylene \rightarrow surface charge-transfer excitations, and above 5 eV there are intra-acetylene excitations.

Acetylene is one of the smallest adsorbates of interest. While this can provide a good model system, it is desirable to study considerably larger molecules. Since the calculation of the $\pi_{\text{C}_2\text{H}_2} \rightarrow \pi_{\text{C}_2\text{H}_2}^*$ excitation in the C₂H₂ + Si₂₁H₂₀ system is already demanding computationally, it is necessary to consider further approximations. In this paper, we adopt the approach of computing excitations within a truncated single excitation space outlined earlier. A variety of truncation schemes can be envisaged. In Table 3 excitation energies computed within a number of schemes are given. For the remainder of this paper, only singlet states are considered.

One of the most severe truncation schemes is to only include excitations from the occupied orbitals localized on the carbon and hydrogen atoms of acetylene (see eq 1). Imposing $\kappa_i^{\text{occ}} = 0.13$ over these atoms resulted in 15 out of the 164 occupied orbitals included in the subspace. Within this scheme, excitations from the π_{Si} orbitals are not observed. The predicted transition energies of excitations from the $\pi_{\text{C}_2\text{H}_2}$ orbital are in reasonable agreement with the values computed within the full single excitation space. However, relatively large errors are introduced for the $\pi_{\text{C}_2\text{H}_2} \rightarrow \pi_{\text{Si}}^*$ excitations. Expanding the excitation space to include additional orbitals associated with the two silicon atoms bonded to carbon (denoted C₂H₂ + 2Si) has very little effect on the computed excitation energies. Similarly, it is also possible to include only excitations from the π_{Si} orbitals. Again, the predicted excitation energies are generally in good agreement with those calculated within the full single excitation space. However, a large error is introduced for the $\pi_{\text{Si}_1} \rightarrow \pi_{\text{Si}_1}^*$ and $\pi_{\text{Si}_2} \rightarrow \pi_{\text{Si}_2}^*$ excitations. These errors arise due to a strong mixing of the transitions with excitations that have been excluded in the restricted excitation space. Combining these schemes and including excitations from orbitals associated with the Si=Si dimers and acetylene results in 43 out of 164 occupied orbitals included. There is a general improvement in the computed excitation energies and the large errors observed previously are reduced substantially. The predicted $\pi_{\text{C}_2\text{H}_2} \rightarrow$

TABLE 4: Predicted Excitation Energies for Benzene on Si₂₁H₂₀

transition	C ₆ H ₆ + Si=Si	C ₆ H ₆
$\pi_{\text{Si}_1} \rightarrow \pi_{\text{Si}_1}^*$	1.69	
$\pi_{\text{Si}_1} \rightarrow \pi_{\text{Si}_2}^*$	2.21 (0.07)	
$\pi_{\text{Si}_1} \rightarrow \pi_1^*$	3.27	
$\pi_{\text{Si}_1} \rightarrow \pi_2^*$	3.58 (0.05)	
$\pi_{\text{Si}_2} \rightarrow \pi_{\text{Si}_1}^*$	1.68	
$\pi_{\text{Si}_2} \rightarrow \pi_{\text{Si}_2}^*$	2.23	
$\pi_{\text{Si}_2} \rightarrow \pi_1^*$	3.29	
$\pi_{\text{Si}_2} \rightarrow \pi_2^*$	3.60	
$\pi_1 \rightarrow \pi_{\text{Si}_1}^*$	2.61 (0.08)	2.55 (0.04)
$\pi_1 \rightarrow \pi_{\text{Si}_2}^*$	2.72	2.70
$\pi_1 \rightarrow \pi_1^*$	4.36 (0.02)	4.36 (0.02)
$\pi_1 \rightarrow \pi_2^*$	4.72	4.72
$\pi_2 \rightarrow \pi_{\text{Si}_1}^*$	3.06	3.13
$\pi_2 \rightarrow \pi_{\text{Si}_2}^*$	3.20 (0.01)	3.29
$\pi_2 \rightarrow \pi_1^*$	4.99	4.98
$\pi_2 \rightarrow \pi_2^*$	5.48 (0.01)	5.46 (0.04)

$\pi_{\text{C}_2\text{H}_2}^*$ excitation energy is in error by less than 0.1 eV. The predicted oscillator strengths tend to be more sensitive to the truncation. Generally, there is an increase in the predicted oscillator strengths. Additional truncation in the virtual space (denoted C₂H₂ + Si=Si*) has little effect on the computed transition energies. Imposing these truncation schemes greatly reduces the computational cost of studying the high-lying excitations localized within organic adsorbates with the introduction of only a relatively small error, particularly when excitations from the orbitals on the adsorbed molecules and the Si=Si dimers are included within the excitation subspace. Consequently, within this approach the excited states of larger adsorbates can be studied.

Benzene Adsorbed on the Si(100) Surface. The most stable structure of benzene adsorbed on Si(100) has been the subject of a number of experimental and theoretical investigations. In a recent study, much of this earlier work was summarized and a comprehensive theoretical study reported.¹¹ The [4+2] structure was found to be the global minimum and this binding configuration is used in the calculations presented here. We are primarily interested in the excitations between the π -like orbitals, these are shown in Figure 4. Similar to acetylene, the HOMO-1, HOMO, LUMO, and LUMO+1 are bonding and antibonding π orbitals localized on the Si=Si dimers. At lower energies, π orbitals associated with the remaining double bonds of the aromatic ring can be identified. These are denoted π_1 and π_2 and are 1.01 and 1.28 eV lower in energy than the HOMO, respectively. At higher energies are corresponding antibonding orbitals π_1^* and π_2^* .

Computed transition energies for excitations between these orbitals are shown in Table 4. Excitation energies within two truncation schemes are shown: truncation of the occupied space

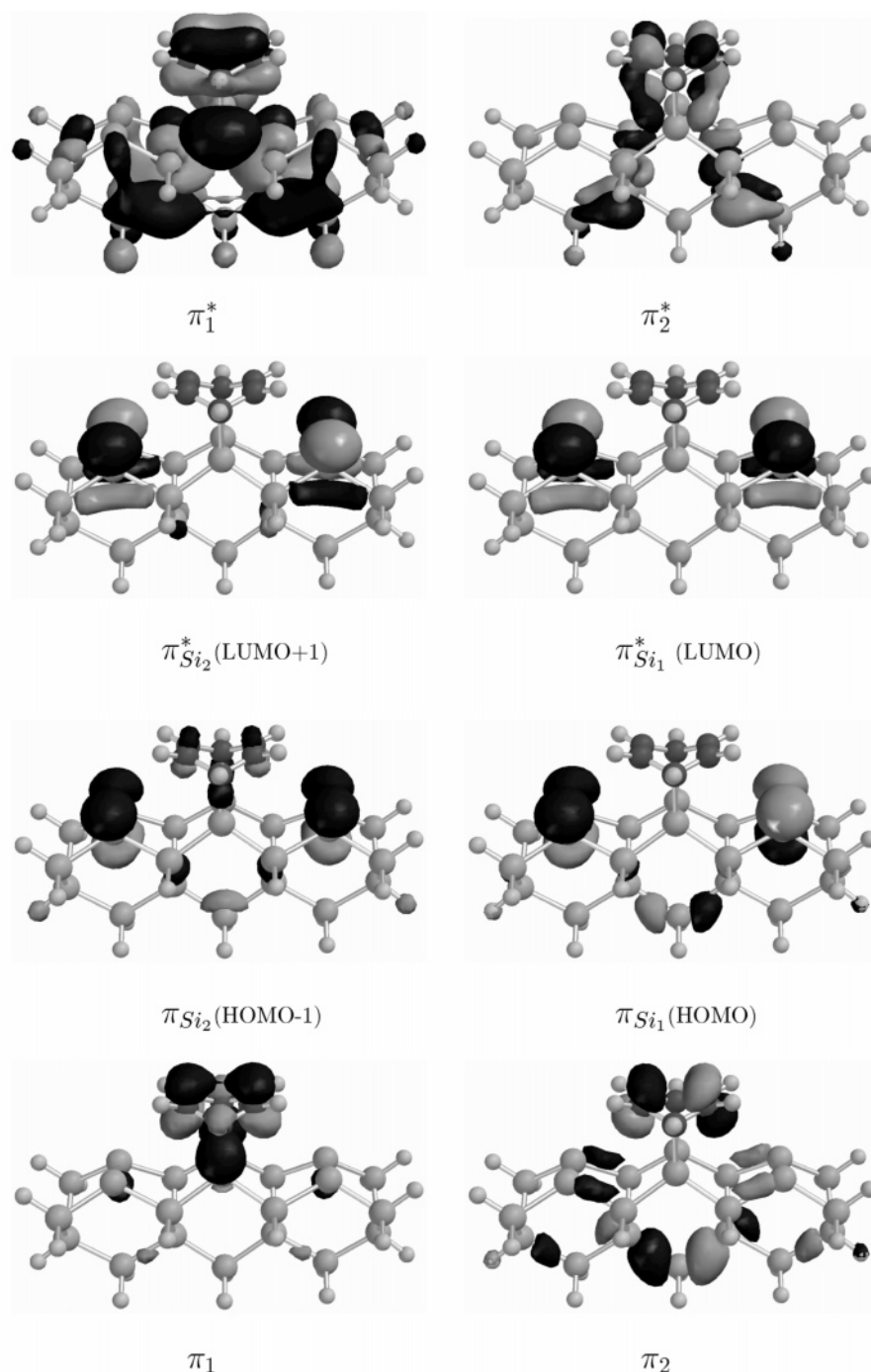


Figure 4. π orbitals of benzene on $\text{Si}_{21}\text{H}_{20}$.

to orbitals associated with benzene and also to benzene with the silicon atoms of the $\text{Si}=\text{Si}$ dimers. Initially we will discuss the results for truncation to the benzene and the silicon dimer orbitals. A pattern similar to the acetylene system emerges. At low excitation energies are the intrasurface $\pi_{\text{Si}} \rightarrow \pi_{\text{Si}}^*$ excitations. These occur at approximately 1.7 and 2.2 eV. Between 2.6 and 4.7 eV are a number of molecule \rightarrow benzene and surface \rightarrow benzene excitations. The π excitations localized within the adsorbed benzene are predicted to lie at 4.99 and 5.48 eV. In gas-phase benzene, the lowest lying valence excited states are the ${}^1\text{L}_b$ and ${}^1\text{L}_a$ excitations. B3LYP/6-31+G* predicts transition energies for these states of 5.42 and 6.28 eV. Similar to acetylene, the excitation energies of the transitions of the adsorbed molecule are lower than those in the gas-phase system.

The study of these excitations within the larger excitation space (including excitations from the silicon dimers) approaches

the limit of the capability of a PC with 2 GB of memory. Imposing the more severe truncation scheme allows the higher lying benzene excitations to be studied more readily. Within this scheme the low-lying excitations from the silicon dimers are no longer observed. However, the predicted excitation energies of the benzene excitations are within 0.05 eV of those from the larger excitation subspace.

9,10-Phenanthrenequinone Adsorbed on the Si(100) Surface. 9,10-Phenanthrenequinone (PQ) has been shown to react with the Si(100) surface through the oxygen atoms, forming a heteroatomic ring.⁵⁷ In contrast to benzene, the aromaticity of PQ is preserved on bonding to the surface. The excited states of PQ adsorbed on Si(100) have become a subject of interest recently due to RDS experiments of Hacker and Hamers.⁴³ Comparison of the RDS spectrum of PQ and 1,2-cyclohexanone on Si(100) showed peaks at 3.3 and 4.2 eV arise through

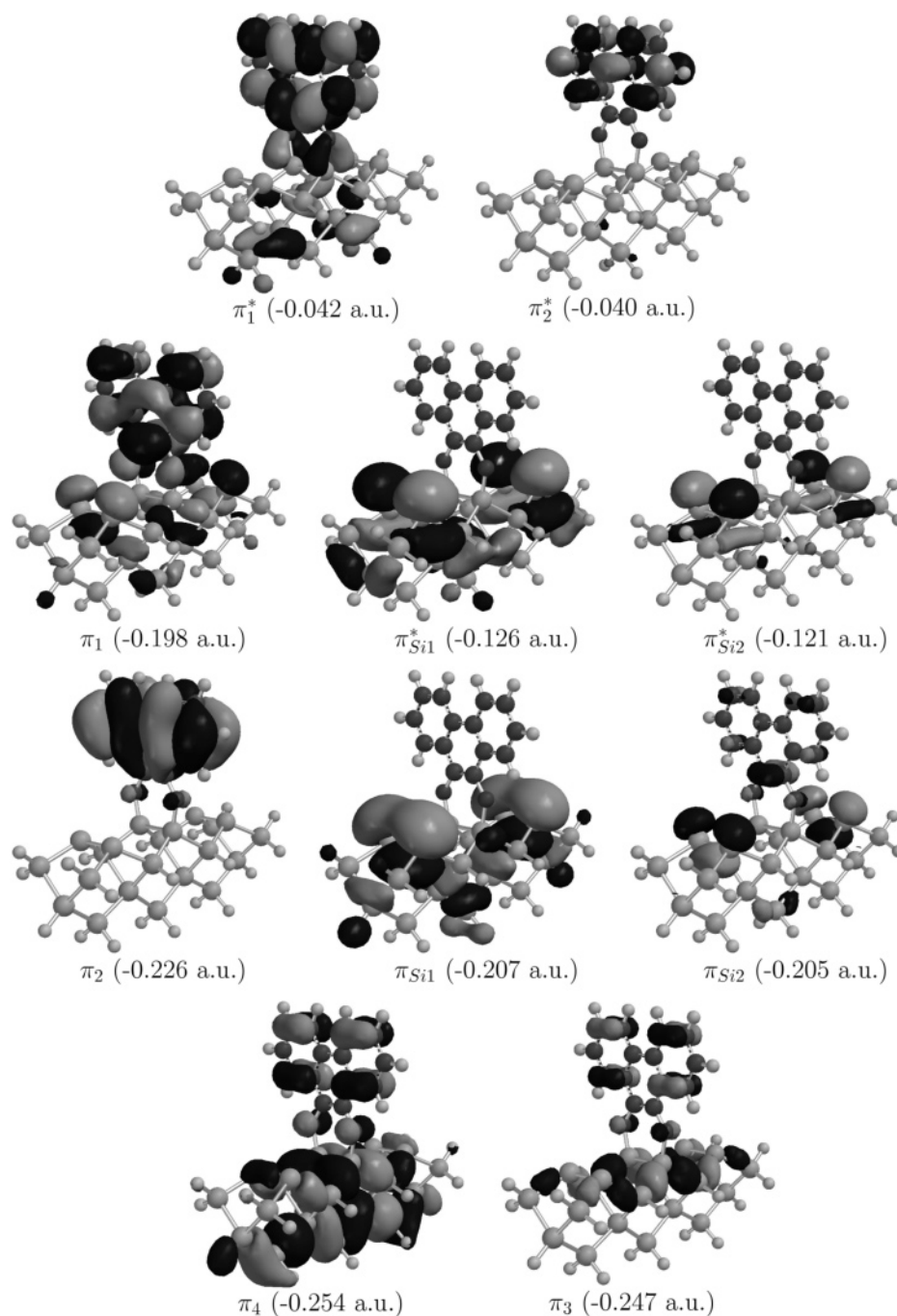


Figure 5. π orbitals of 9,10-phenanthrenequinone on $\text{Si}_{21}\text{H}_{20}$.

surface termination induced perturbation of the bulk reflectivity. Furthermore, a new feature in the spectrum at 5.2 eV was assigned to $\pi\pi^*$ transitions within the aromatic rings of PQ. Subsequent theoretical simulation of the RDS spectrum based on plane wave GGA-DFT calculations indicated that the 5.2 eV feature does not arise from intramolecular PQ excitations.^{44,45} Both groups provide convincing arguments to support their conclusions and the nature of this transition remains unclear. Through calculation of the electronic excited states it is possible to determine in which regions of the spectrum the intramolecular and charge-transfer excitations of PQ should arise.

Our calculations are based on PQ standing vertically and bonded to the central Si=Si dimer of the $\text{Si}_{21}\text{H}_{20}$ cluster (C_{2v} symmetry). The π -like orbitals with associated energies are shown in Figure 5. The adsorption of PQ shows qualitative differences to acetylene and benzene. The HOMO (π_1) is

predominantly a π orbital of PQ. Although there is some contribution from the π orbitals of the Si=Si dimer, below this orbital are the π orbitals that are predominantly localized on the Si=Si dimers. However, for this system the distinction is less clear since the $\pi_{\text{Si}2}$ orbital does contain contributions from PQ. At lower energies are further π orbitals that are localized on the aromatic rings of PQ. The LUMO ($\pi_{\text{Si}1}^*$) and LUMO+1 ($\pi_{\text{Si}2}^*$) orbitals are clearly π^* orbitals associated with the silicon dimers. At significantly higher energies are the π^* orbitals of PQ, labeled π_1^* and π_2^* .

Computed excitation energies for PQ on Si_9H_{12} and $\text{Si}_{21}\text{H}_{20}$ clusters are shown in Table 5. For PQ on Si_9H_{12} , intermolecular excitations between surface and PQ are not observed. Molecular PQ $\pi\pi^*$ excitations are predicted to occur at ~ 4 , ~ 4.65 , ~ 5.25 , and ~ 5.55 eV. Further $\pi\pi^*$ transitions from lower lying π orbitals will occur at higher energies. For calculations on the

TABLE 5: Predicted Excitation Energies for 9,10-Phenanthrenequinone on Si(100) and Gas-Phase 9,10-Phenanthrenequinone at the Optimized and Adsorbed Structures^a

transition	Si ₉ H ₁₂ full	Si ₂₁ H ₂₀		gas phase	
		full	truncated	optimized	adsorbed
$\pi_1 \rightarrow \pi^*_{\text{Si}_1}$		1.53	1.53		
$\pi_1 \rightarrow \pi^*_{\text{Si}_2}$		1.66	1.66		
$\pi_1 \rightarrow \pi^*_1$	4.07 (0.08)	3.83	3.83		
$\pi_1 \rightarrow \pi^*_2$	3.92 (0.01)	3.84	3.80 (0.01)		
$\pi_{\text{Si}_2} \rightarrow \pi^*_{\text{Si}_1}$		1.78	1.78		
$\pi_{\text{Si}_2} \rightarrow \pi^*_{\text{Si}_2}$		1.84	1.84		
$\pi_{\text{Si}_2} \rightarrow \pi^*_1$		4.05 (0.04)	4.38		
$\pi_{\text{Si}_2} \rightarrow \pi^*_2$		4.13	3.99		
$\pi_{\text{Si}_1} \rightarrow \pi^*_{\text{Si}_1}$		2.16 (0.06)	2.23 (0.07)		
$\pi_{\text{Si}_1} \rightarrow \pi^*_{\text{Si}_2}$		2.18	2.26		
$\pi_{\text{Si}_1} \rightarrow \pi^*_1$		4.01	4.01		
$\pi_{\text{Si}_1} \rightarrow \pi^*_2$		4.03	4.10		
$\pi_2 \rightarrow \pi^*_{\text{Si}_1}$		2.32	2.32		
$\pi_2 \rightarrow \pi^*_{\text{Si}_2}$		2.45	2.46		
$\pi_2 \rightarrow \pi^*_1$	4.60 (0.07)	4.58 (0.06)	4.43 (0.24)	4.93 (0.01)	4.69 (0.08)
$\pi_2 \rightarrow \pi^*_2$	4.70 (0.04)	4.54 (0.01)	4.50	4.95 (0.52)	4.70 (0.14)
$\pi_3 \rightarrow \pi^*_{\text{Si}_1}$		2.71 (0.02)	2.72 (0.03)		
$\pi_3 \rightarrow \pi^*_{\text{Si}_2}$		2.84	2.85		
$\pi_3 \rightarrow \pi^*_1$	5.19 (0.03)	n/a	5.16 (0.02)	5.87 (0.21)	5.50 (0.05)
$\pi_3 \rightarrow \pi^*_2$	5.34 (0.36)	n/a	5.22 (0.06)	5.25 (0.02)	5.06 (0.01)
$\pi_4 \rightarrow \pi^*_{\text{Si}_1}$		2.89	2.90		
$\pi_4 \rightarrow \pi^*_{\text{Si}_2}$		3.04	3.04 (0.06)		
$\pi_4 \rightarrow \pi^*_1$	5.51	n/a	5.31 (0.10)	5.92 (0.06)	5.49 (0.05)
$\pi_4 \rightarrow \pi^*_2$	5.63	n/a	5.61 (0.17)	5.92 (0.15)	5.71 (0.31)

^a n/a: not available due to cost of calculation.

larger cluster, there are a number of low-lying excitations (1.5–3 eV) to the π^* orbitals of the Si=Si dimers, with intrasurface excitations at 1.8 and 2.2 eV. $\pi\pi^*$ excitations within the aromatic ring are predicted to occur at 3.8, 4.5, and 4.6 eV. These are a little lower than the corresponding excitations of the Si₉H₁₂ cluster. For the larger cluster, the higher lying $\pi\pi^*$ states could not be computed due to the computational cost. These roots are not among the lowest 150 roots. To explore the higher lying excited states of the aromatic ring we impose a restriction on the size of the single excitation space. The occupied π of PQ orbitals are relatively high in energy and little computational advantage is gained from truncation within the occupied space. The PQ virtual π^* orbitals are high in energy and, consequently, for this system it is beneficial to impose truncation within the virtual space. Excitation energies for the calculation in which only excitations to the π^* orbitals shown in Figure 5 in addition to a further π^* orbital of PQ are included. The resulting excitation energies are generally close to those from the full excitation space. This is quite surprising since this represents a severe restriction. However, for some transitions a significant error is introduced. The predicted excitation energies of the higher $\pi\pi^*$ states are 5.16, 5.22, 5.31, and 5.61 eV. Through inspection of the molecular orbitals of PQ in the gas phase, corresponding excitations can be identified. These excitation energies are also shown in Table 5. There is a large shift to lower energies on adsorption. Also shown are excitation energies of PQ computed at the structure of the adsorbed species. These excitation energies are closer to those obtained for PQ on the Si(100) clusters. This indicates that the shifts arise in part from structural changes that occur upon adsorption.

The calculations clearly indicate that there are $\pi\pi^*$ excitations of the aromatic ring around 5.2 eV. However, the calculations cannot be related directly to RDS measurements since no prediction of the sign or magnitude of the RDS intensity is made. In this region of the spectrum are also a number of excitations from within the cluster to the π^* orbitals of PQ. It is possible that these excitations will also contribute to the band at 5.2 eV.

Conclusions

The calculation of the excited states of molecules adsorbed on surfaces represents a severe challenge to theoretical chemistry. This study has shown how the excited states of organic molecules adsorbed on the Si(100) surface can be computed within a TDDFT formalism. Computation of the relatively high lying intraadsorbate excitations can be achieved by performing the TDDFT calculation within a subspace of the single excitations. This work has focused on excitations between the π -like orbitals. To minimize the error introduced by this truncation it is beneficial to include excitations from the occupied orbitals associated with the silicon atoms of the Si=Si dimers, in addition to those of the adsorbed molecule. The resulting excitation energies will not be exact or represent “benchmark” calculations. Calculations of very high accuracy such as MRCI with large basis sets will not be possible for this type of system soon. However, the results are sufficient for a general picture of the excited states to be established.

For clean Si(100) the low-lying excitations correspond to electronic excitations between the π orbitals of the Si=Si dimers. On an extended surface there will be a very large number of these excitations, which the calculations predict to lie in the range 0.4–2 eV for the triplet states and 1.1–2.25 eV for the singlet states. The triplet excitations are spin forbidden and so the corresponding intensities are zero. However, some of the singlet excitations do have significant oscillator strengths. For adsorbed acetylene and benzene, intrasurface, charge transfer, and intramolecule excitations can be identified. At low energies are the remaining excitations between the occupied and virtual orbitals of the silicon dimers. Above these excitations are surface \rightarrow molecule and molecule \rightarrow surface charge-transfer excitations. At higher energies are the intramolecule excitations between the remaining π orbitals of the adsorbed molecule. These excitations occur at lower energies than corresponding excitations of the molecule in the gas phase. For PQ adsorbed on Si(100), $\pi\pi^*$ excitations of the aromatic ring of PQ are predicted

to occur at 3.8, 4.5, 5.2, 5.3, and 5.6 eV. These are consistent with previous theoretical predictions. Despite the aromaticity of PQ remaining intact on adsorption, these excitation energies are shifted significantly from the gas-phase values. These shifts arise in part from changes in the structure that occur. While $\pi\pi^*$ excitations are found at 5.2 eV, direct assignment of the peak in RDS measurements cannot be made. In this region of the spectrum excitations from the clusters to the π^* orbitals of PQ are also observed, which may also contribute to the RDS spectrum in this region.

Acknowledgment. This work was supported by the Engineering and Physical Sciences Research Council (UK) through the award of an Advanced Research Fellowship (GR/R77636) to N.A.B.

References and Notes

- (1) Konecny, R.; Doren, D. J. *J. Am. Chem. Soc.* **1997**, *119*, 11098.
- (2) McEllistrem, M.; Allgeier, M.; Boland, J. J. *Science* **1998**, *279*, 545.
- (3) Barriocanal, J. A.; Doren, D. J. *J. Phys. Chem. B* **2000**, *104*, 12269.
- (4) Lopinski, G. P.; Wayner, D. D. M.; Wolkow, R. A. *Nature* **2000**, *406*, 48.
- (5) Buehler, E. J.; Boland, J. J. *Science* **2000**, *290*, 506.
- (6) Hofer, W. A.; Fisher, A. J.; Lopinski, G. P.; Wolkow, R. A. *Phys. Rev. B* **2001**, *63*, 085314.
- (7) Ho Choi, C.; Liu, D.-J.; Evans, J. W.; Gordon, M. S. *J. Am. Chem. Soc.* **2002**, *124*, 8730.
- (8) Ho Choi, C.; Gordon, M. S. *J. Am. Chem. Soc.* **2002**, *124*, 6162.
- (9) Phillips, M. A.; Besley, N. A.; Gill, P. M. W.; Moriarty, P. *Phys. Rev. B* **2003**, *67*, 035309.
- (10) Rintelman, J. M.; Gordon, M. S. *J. Phys. Chem. B* **2004**, *108*, 7820.
- (11) Jung, Y.; Gordon, M. S. *J. Am. Chem. Soc.* **2005**, *127*, 3131.
- (12) Lastapis, M.; Martin, M.; Riedel, D.; Hellner, L.; Comlet, G.; Dujardin, G. *Science* **2005**, *308*, 1000.
- (13) Chen, J.; Reed, M. A.; Rawlett, A. M.; Tour, J. M. *Science* **1999**, *286*, 1550.
- (14) Donhauser, Z. J.; Mantooh, B. A.; Kelly, K. F.; Brumm, L. A.; Monnell, J. D.; Stapleton, J. J.; Price, D. W., Jr.; Rawlett, A. M.; Allara, D. L.; Tour, J. M.; Weiss, P. S. *Science* **2001**, *292*, 2303.
- (15) Schon, J. H.; Meng, H.; Bao, Z. *Science* **2001**, *294*, 2138.
- (16) Paulus, B. *Surf. Sci.* **1998**, *408*, 195.
- (17) Himpel, F. J.; Heimann, P.; Chang, T.-C.; Eastman, D. E. *Phys. Rev. Lett.* **1980**, *45*, 1112.
- (18) Johansson, L. S. O.; Uhrberg, R. I. G.; Martensson, P.; Hansson, G. V. *Phys. Rev. B* **1990**, *42*, 1305.
- (19) Wertheim, G. K.; Riffe, D. M.; Rowe, J. E.; Citrin, P. H. *Phys. Rev. Lett.* **1991**, *67*, 120.
- (20) Landemark, E.; Karlsson, C. J.; Chao, Y.-C.; Uhrberg, R. I. G. *Phys. Rev. Lett.* **1992**, *69*, 1588.
- (21) Shkrebtii, A. I.; Del Sole, R. *Phys. Rev. Lett.* **1993**, *70*, 2645.
- (22) Hamers, R. J.; Tromp, R. M.; Demuth, J. E. *Phys. Rev. B* **1986**, *34*, 5343.
- (23) Wolkow, R. A. *Phys. Rev. Lett.* **1992**, *68*, 2636.
- (24) Kondo, Y.; Amakusa, T.; Iwatsuki, M.; Tokumoto, H. *Surf. Sci.* **2000**, *453*, L318.
- (25) Shoemaker, J.; Burggraf, L. W.; Gordon, M. S. *J. Chem. Phys.* **2000**, *112*, 2994.
- (26) Gordon, M. S.; Shoemaker, J.; Burggraf, L. W. *J. Chem. Phys.* **2000**, *113*, 9355.
- (27) Hess, J. S.; Doren, D. J. *J. Chem. Phys.* **2000**, *113*, 9353.
- (28) Yung, Y.; Shao, Y.; Gordon, M. S.; Doren, D. J.; Head-Gordon, M. *J. Chem. Phys.* **2003**, *119*, 10917.
- (29) Hamers, R. J.; Avouris, P.; Bozso, F. *Phys. Rev. Lett.* **1987**, *59*, 2071.
- (30) Pan, W.; Zhu, T.; Yang, W. *J. Chem. Phys.* **1997**, *107*, 3981.
- (31) Lopinski, G. P.; Moffatt, D. J.; Wolkow, R. A. *Chem. Phys. Lett.* **1998**, *282*, 305.
- (32) Qiao, M. H.; Cao, Y.; Tao, F.; Liu, Q.; Deng, J. F.; Xu, G. Q. *J. Phys. Chem. B* **2000**, *104*, 11211.
- (33) Besley, N. A. *Chem. Phys. Lett.* **2004**, *390*, 124.
- (34) Besley, N. A. *J. Chem. Phys.* **2005**, *122*, 184706.
- (35) Frederick, B. G.; Power, J. R.; Cole, R. J.; Perry, C. C.; Chen, Q.; Haq, S.; Bertrams, T.; Richardson, N. V.; Weightman, P. *Phys. Rev. Lett.* **1998**, *80*, 4490.
- (36) Hess, J. S.; Doren, D. J. *J. Phys. Chem. B* **2002**, *106*, 8206.
- (37) Benedict, L. X.; Puzder, A.; Williamson, A. J.; Grossman, J. C.; Galli, G.; Klepeis, J. E.; Raty, J.-Y.; Pankratov, O. *Phys. Rev. B* **2003**, *68*, 085310.
- (38) Aspnes, D. E.; Studna, A. A. *Phys. Rev. Lett.* **1985**, *54*, 1956.
- (39) Yasuda, T.; Mantese, L.; Rossow, U.; Aspnes, D. E. *Phys. Rev. Lett.* **1995**, *74*, 3431.
- (40) Kipp, L.; Biegelsen, D. K.; Northrup, J. E.; Swartz, L.-E.; Bringans, R. D. *Phys. Rev. Lett.* **1996**, *76*, 2810.
- (41) Cole, R. J.; Tanaka, S.; Gerber, P.; Power, J. R.; Farrell, T.; Weightman, P. *Phys. Rev. B* **1996**, *54*, 13444.
- (42) Shioda, R.; van der Weide, J. *Phys. Rev. B* **1998**, *57*, R6823.
- (43) Hacker, C. A.; Hamers, R. J. *J. Phys. Chem. B* **2003**, *107*, 7689.
- (44) Hermann, A.; Schmidt, W. G.; Bechstedt, F. *Phys. Rev. B* **2005**, *71*, 153311.
- (45) Hermann, A.; Schmidt, W. G.; Bechstedt, F. *J. Phys. Chem. B* **2005**, *109*, 7928.
- (46) Tozer, D. J.; Amos, R. D.; Handy, N. C.; Roos, B. O.; Serrano-Andres, L. *Mol. Phys.* **1999**, *97*, 859.
- (47) Mulliken, R. S. *J. Chem. Phys.* **1955**, *23*, 1833.
- (48) Stephens, P. J.; Devlin, F. J.; Chabalowski, C. F.; Frisch, M. J. *J. Phys. Chem.* **1994**, *98*, 11623.
- (49) Hehre, W. J.; Ditchfield, R.; Pople, J. A. *J. Chem. Phys.* **1972**, *56*, 294.
- (50) Hariharan, P. C.; Pople, J. A. *Theor. Chim. Acta* **1973**, *28*, 213.
- (51) Wang, Y.; Shi, M.; Rabalais, J. W. *Phys. Rev. B* **1993**, *48*, 1689.
- (52) Hirata, S.; Head-Gordon, M. *Chem. Phys. Lett.* **1999**, *17*, 291.
- (53) Kong, J.; White, C. A.; Krylov, A. I.; Sherrill, C. D.; Adamson, R. D.; Furlani, T. R.; Lee, M. S.; Lee, A. M.; Gwaltney, S. R.; Adams, T. R.; Ochsenfeld, C.; Gilbert, A. T. B.; Kedziora, G. S.; Rassolov, V. A.; Maurice, D. R.; Nair, N.; Shao, Y.; Besley, N. A.; Maslen, P. E.; Dombroski, J. P.; Dachselt, H.; Zhang, W. M.; Korambath, P. P.; Baker, J.; Byrd, E. F. C.; Van Voorhis, T.; Oumi, M.; Hirata, S.; Hsu, C. P.; Ishikawa, N.; Florian, J.; Warshel, A.; Johnson, B. G.; Gill, P. M. W.; Head-Gordon, M.; Pople, J. A. *J. Comput. Chem.* **2000**, *21*, 1532.
- (54) Dreuw, A. D.; Weisman, J. L.; Head-Gordon, M. *J. Chem. Phys.* **2003**, *119*, 2943.
- (55) Iikura, H.; Tsuneda, T.; Yanai, T.; Hirao, K. *J. Chem. Phys.* **2001**, *115*, 3540.
- (56) Tawada, Y.; Tsuneda, T.; Yanagisawa, S.; Yanai, T.; Hirao, K. *J. Chem. Phys.* **2004**, *120*, 8425.
- (57) Fang, L.; Liu, J.; Coulter, S.; Cao, X.; Schwartz, M. P.; Hacker, C. A.; Hamers, R. J. *Surf. Sci.* **2002**, *514*, 362.